

# Auxetic properties of a newly proposed $\gamma$ -graphyne-like material

Ricardo Paupitz<sup>a</sup>, Tales J. da Silva<sup>b</sup>, Marilia J. Caldas<sup>b</sup>, Douglas S. Galvão<sup>c</sup>, Alexandre F. Fonseca<sup>c</sup>

<sup>a</sup>*Physics Department, São Paulo State University - UNESP, 13506-900, Rio Claro, SP, Brazil.*

<sup>b</sup>*Institute of Physics, University of São Paulo, CEP 05508-090, São Paulo, SP, Brazil.*

<sup>c</sup>*Applied Physics Department, Institute of Physics “Gleb Wataghin”, State University of Campinas, Campinas, SP, 13083-970, Brazil.*

---

## Abstract

In this work, we propose a new auxetic (negative Poisson’s ratio values) structure, based on a  $\gamma$ -graphyne structure, here named *A $\gamma$ G structure*. Graphynes are 2D carbon allotropes with phenylic rings connected by acetylenic groups. The A $\gamma$ G structural/mechanical and electronic properties, as well as its thermal stability, were investigated using classical reactive and quantum molecular dynamics simulations. We found that A $\gamma$ G has a large bandgap of 2.48 eV and is thermally stable at a large range of temperatures. It presents a Young’s modulus that is an order of magnitude smaller than that of graphene or  $\gamma$ -graphyne. The classical and quantum results are consistent and validate that the A $\gamma$ G is auxetic, both when isolated (vacuum) and when deposited on a copper substrate. We believe that this is the densest auxetic structure belonging to the graphyne-like families.

**Keywords:** Carbon materials, Elastic properties, Simulation and modelling

---

## 1. Introduction

Auxeticity is an interesting but unusual mechanical property only present in few materials. Auxetic materials transversely expand (contract) when longitudinally stretched (compressed) [1, 2]. They are characterized by negative values of the Poisson ratio,  $\nu$ , defined as  $\nu = -\epsilon_y/\epsilon_x$ , where  $\epsilon_y$  ( $\epsilon_x$ ) is the transverse (longitudinal) strain in response to the applied longitudinal stress [3]. Poisson ratio values are usually positive while being negative for auxetic materials [4–8]. Zero, or close to zero values are even more rare [9–12].

Auxeticity in nanomaterials has been object of intense research [13, 14]. In particular, several studies of molecular and/or polymer networks with negative and/or zero Poisson’s ratio are found in the literature [7, 10, 15–23]. As the Poisson ratio is scale-independent, a structure possessing negative or zero Poisson’s ratio at molecular level is expected to manifest this property at macroscopic scale.

Graphynes are two-dimensional one-atom-thick carbon allotropes. Their structures can be formed by any possible combination of connected acetylenic ( $-\text{C}\equiv\text{C}-$ ) groups not only to each other but also to phenylic rings and/or carbon-carbon bonds, thus generating different families of structures [24–26]. Graphyne-based structures present electronic [27], thermal [28–30] and mechanical [30–33] properties that make them suitable

for a series of different applications.

Most of the graphyne-based structures have positive Poisson’s ratio values [30], however, in the last decades, some auxetic structures were reported in the literature. Evans and collaborators [4, 10, 21] reported the auxeticity of reentrant poly-phenylacetylene networks, called *reflexynes*. Grima and Evans [20] showed that networks of acetylenic polytriangles with benzene rings at the vertices, named as *polytriangles-n-yne*s, with  $n$  being the number of acetylenic linkages, are also auxetic for  $n \geq 2$ .

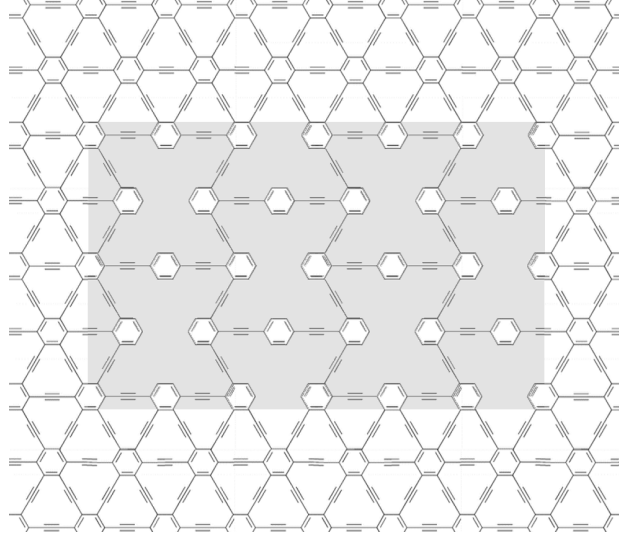


Figure 1: The newly proposed auxetic  $\gamma$ -graphyne-like, ( $A\gamma G$ ) is shown in the gray area. For reference, its parent regular  $\gamma$ -graphyne, in the non-gray area, is also shown. See text for discussions.

In this work, we report the design and investigation of the electronic and mechanical properties of a newly proposed  $\gamma$ -graphyne-based auxetic structure, that we name as *auxetic  $\gamma$ -graphyne-like* ( $A\gamma G$ ), shown in the grey area of Fig. 1. For reference, its parent  $\gamma$ -graphyne (non-grey area) is also shown, in order to indicate how the auxetic structure was obtained, which is by ‘deleting’ specific acetylenic arms from a regular  $\gamma$ -graphyne, thus creating a reentrant-like structure. The resulting carbon atoms with dangling bonds are then hydrogen passivated (for clarity, these hydrogen atoms are not shown in Fig. 1). The elastic properties were obtained for the infinite isolated  $A\gamma G$  layer, as well as for one finite structure on a copper substrate. The thermal stability of this structure was also tested to rule out the possibility of thermally induced scrolling and/or folding.

## 2. Computational Details

Density Functional based Tight Binding (DFTB) and classical molecular dynamics (MD) simulations were carried out to investigate the structural stability, mechanical and thermal properties of the  $A\gamma G$ . The geometry optimization of the structures was performed by energy minimization through a conjugate-gradient

algorithm implemented in the LAMMPS code [34], with a force tolerance set to  $10^{-8}$  eV/Å. Thermal stability was simulated with a Langevin thermostat using a damping factor set to 1 ps.

The in-plane elastic properties of an infinite A $\gamma$ G structure was evaluated through [35] the following equation:

$$U(\varepsilon) = \frac{1}{2}C_{11}\varepsilon_{xx}^2 + \frac{1}{2}C_{22}\varepsilon_{yy}^2 + C_{12}\varepsilon_{xx}\varepsilon_{yy}, \quad (1)$$

where  $U$  is the energy per area of the 2D structure, and  $\varepsilon_{xx}$  and  $\varepsilon_{yy}$  are the strains along the  $x$  and  $y$  directions, respectively. With the values of  $C_{11}$ ,  $C_{12}$  and  $C_{22}$ , the Young's modulus,  $Y$ , the Poisson's ratio,  $\nu$ , and the linear compressibility,  $\beta$ , along two in-plane directions, can be calculated:  $Y_x = (C_{11}C_{22} - C_{12}^2)/C_{22}$ ,  $Y_y = Y_x C_{22}/C_{11}$ ,  $\nu_{xy} = C_{12}/C_{22}$ ,  $\nu_{yx} = C_{12}/C_{11}$ ,  $\beta_x = (C_{22} - C_{12})/K$  and  $\beta_y = (C_{11} - C_{12})/K$ , with  $K \equiv (C_{11}C_{22} - C_{12}^2)$ .

$C_{ij}$ ,  $i, j = 1, 2$ , were obtained from two uniaxial tensile tests (one along each direction) and one biaxial tensile test. The uniaxial tensile test consists of pulling the structure along the  $x$  ( $y$ ) direction while keeping its size along  $y$  ( $x$ ) direction fixed or imposing  $\varepsilon_{yy} = 0$  ( $\varepsilon_{xx} = 0$ ). The biaxial test consists of pulling the structure along the  $x$  and  $y$  directions at the same time and by the same amount of strain ( $\varepsilon_{xx} = \varepsilon_{yy} \equiv \varepsilon$ ).  $C_{11}$  ( $C_{22}$ ) is obtained from an uniaxial tensile test, where Eq. (1) becomes  $U(\varepsilon) = 0.5C_{11}\varepsilon^2$  ( $U(\varepsilon) = 0.5C_{22}\varepsilon^2$ ), that is further fitted for  $U$  versus uniaxial  $\varepsilon$ .  $C_{12}$  is obtained from a biaxial test, where Eq. (1) becomes  $U(\varepsilon) = M\varepsilon^2$ , where  $M = C_{12} + 0.5(C_{11} + C_{22})$ , that is further fitted for  $U$  versus biaxial  $\varepsilon$ .

Strain increments of 0.1%, from 0 up to 1%, were applied to the A $\gamma$ G structure under periodic boundary conditions, which is consistent with the type of tensile test simulated. Energies per area,  $U$ , were collected from the results of energy minimization as described above, using three force-fields (AIREBO [36], COMB3 [37] and ReaxFF [38, 39]) and the DFTB method (described ahead) in order to verify if the mechanical properties (and, in particular, the auxeticity of the structure) are potential or method dependent. AIREBO, COMB3, and ReaxFF are three of the most used MD potentials to the study of structural and mechanical properties of carbon and other nanostructures. The ReaxFF parameters used here are from Mueller *et al.* [39]. Fittings of the data by a parabolic function on  $\varepsilon$  were performed to obtain  $C_{ij}$ ,  $i, j = 1, 2$  and, from them, the corresponding Young's moduli, Poisson's ratio, and linear compressibility values.

The electronic structure calculations were carried within the DFTB approximation, which can be described as a combination of Density Functional Theory (DFT) and Tight Binding [40, 41] methods. This approximation allows quantum simulations of the electronic and structural properties for relatively large systems combining, as much as possible, the low computational cost of tight-binding methods with the known precision of DFT [42]. In order to achieve this optimized performance, DFTB is based on a second-order expansion of the Kohn-Sham energy defined in DFT [43]. In the present work we adopted the self consistent charge (SCC)-DFTB version, as implemented in DFTB+ code [44, 45] and the *matsci* parametrization [44, 46–48]. For the infinite structure cyclic boundary conditions were adopted in the  $x, y$  directions,

Table 1: Elastic constants  $C_{ij}$  (GPa.nm), Young’s modulus  $Y$  (GPa.nm), Poisson’s ratio  $\nu$  and linear compressibility  $\beta$  (GPa.nm) $^{-1}$  of the A $\gamma$ G from different methods and MD potentials.

Method	$C_{11}$	$C_{22}$	$C_{12}$	$Y_x$	$Y_y$	$\nu_{xy}$	$\nu_{yx}$	$\beta_x$	$\beta_y$
MD AIREBO	40.28	31.48	-26.40	18.13	14.17	-0.84	-0.66	0.101	0.117
MD COMB3	29.14	19.16	-16.47	14.99	9.85	-0.86	-0.57	0.124	0.159
MD ReaxFF	31.16	32.60	-23.00	14.93	15.62	-0.71	-0.74	0.114	0.111
DFTB	42.41	33.83	-26.44	21.74	17.34	-0.78	-0.62	0.082	0.094

with enough distance along  $z$  to avoid interaction between layers. Geometrical optimizations were performed considering a conjugate gradient algorithm in which the convergence for geometry was achieved with a maximum force difference of  $10^{-6}$  and SCC iterations with a maximum tolerance of  $10^{-6}$ . Quantum Molecular Dynamics simulations for several temperatures were performed with the Verlet algorithm and under the control of a Nose-Hoover Thermostat [49], as implemented in DFTB+ software [45]. Atomic structure visualizations and the snapshots combined in the movies (see the Supplementary Materials) were obtained with the VMD software [50].

### 3. Results and Discussion

In Table 1 we present the results for the elastic constants,  $C_{ij}$  (GPa.nm), Young’s modulus,  $Y$  (GPa.nm), Poisson’s ratio,  $\nu$ , and linear compressibility,  $\beta$  (GPa.nm) $^{-1}$ , of the A $\gamma$ G from the simulations with the MD potentials and DFTB. All results are consistent with relation to the fact that A $\gamma$ G is auxetic, with Poisson’s ratio values between -0.57 and -0.86. For the Young’s modulus of A $\gamma$ G, DFTB values are among the stiffest, with  $Y_x = 21.74$  (GPa.nm) being the highest value found, while  $Y_y = 9.85$  (GPa.nm) obtained from COMB3 is the smallest. One remarkable difference is that ReaxFF predicts symmetric behavior of the elastic properties of A $\gamma$ G, while AIREBO and COMB3 predict asymmetric behavior. Also, results from DFTB predict asymmetric behavior of the elastic properties, with absolute values closer to those from the AIREBO potential.

The lattice vectors used to define the 2-dimensional Bravais lattice, as well as the DFTB+ results for the density of states (DOS) and band structure, are shown in Figure 2. The direct bandgap, around 2.48 eV, is located at the M point and suggests that the structure would behave as an insulator or a wide bandgap semiconductor. The DOS analysis confirms that, as expected, the top valence and lowest conduction band states are formed by mainly contributions from the 2p ( $\pi$ ) carbon orbitals. On the other hand, the small dispersion/curvature observed at the bottom of the conduction band and on the top of the valence band indicates charge carriers with relatively large effective masses.

The thermal stability of A $\gamma$ G structures was verified through MD simulations. The isolated structures (in

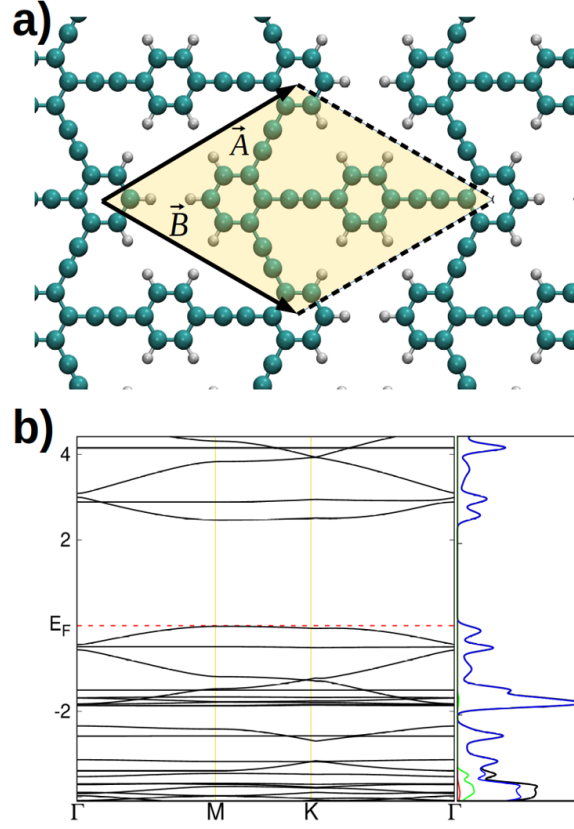


Figure 2: a) The unit cell of the A $\gamma$ G structure is indicated by the yellow area. The lattice vectors  $\vec{A}$  and  $\vec{B}$  have the same length ( $\|\vec{A}\| = \|\vec{B}\| = 12.12 \text{ \AA}$ ) and forming a  $60^\circ$  angle. Cyan and white spheres represent carbon and hydrogen atoms, respectively. b) DFTB band structure and DOS.  $E_F$  is the Fermi level energy, highlighted by the red dashed line. Blue and green lines indicate the  $p$  and  $s$  orbital contributions from carbon atoms to the total density of states, while the red solid line shows the  $s$  orbital contribution originated from the hydrogen atoms. The black line indicates the total density of states.

vacuum) were simulated at room temperature using either classical or quantum MD methods. DFTB based MD simulations suggest that the structure remains stable at room temperature. For high temperatures, there were deformations but with no bond breaking up to 1000 K in vacuum conditions (videos S1 and S2 in the supplementary material).

We have also carried classical MD simulations to test the thermal stability of a finite A $\gamma$ G structure (of about  $63 \times 60 \text{ \AA}$  of size, see right panel of Fig. 3) deposited on a copper substrate. The structure is very stable at 300 K, but for high temperatures (about 1000 K), some atoms from the borders detach off the substrate after 200 ps (data not shown).

Dynamical tensile strain tests were then simulated for the finite, hydrogen-passivated, A $\gamma$ G structure, in order to verify its auxeticity at room temperature and deposited on the copper substrate (see right panel

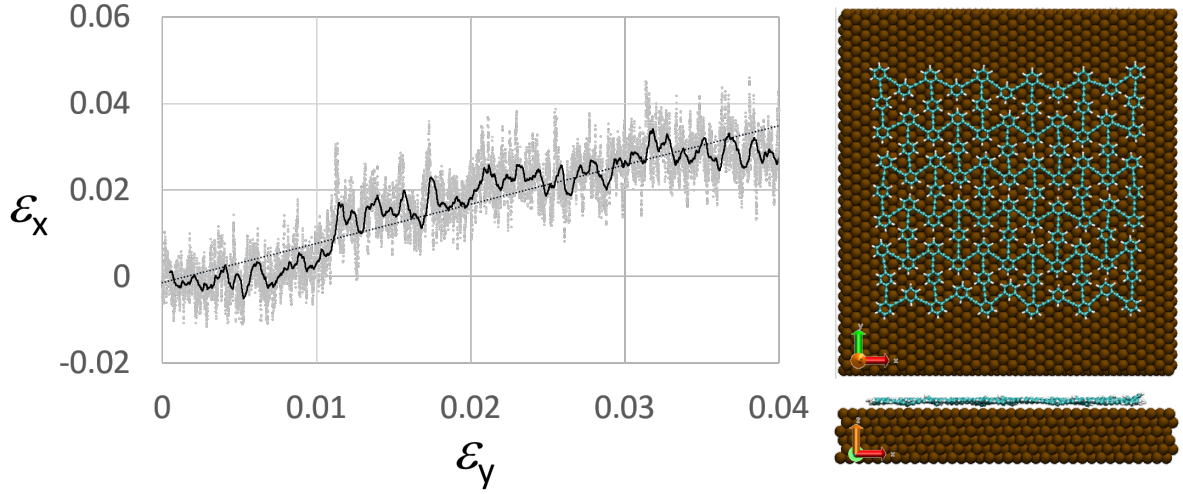


Figure 3: Left panel: variation of the strain of the  $63 \times 60 \text{ \AA}$   $A\gamma G$  structure on a copper substrate along the  $x$  direction, as a function of the applied strain along the  $y$  direction. Gray dots are raw data from the MD simulations. The black curve and black dotted line represent the average curve (made with 255 points), and the linear fitting of the data, respectively. Right panel: upper and lateral views of the structure.

of Fig. 3). The COMB3 potential was used to simulate this configuration. Strain along the  $x$  direction,  $\varepsilon_x$ , was collected as a function of the strain along the  $y$  direction,  $\varepsilon_y$ , that was the direction of the applied tensile pulling stress. The carbon atoms at the bottom edge of the structure were fixed and the carbon atoms at the uppermost edge of the structure were moved along the  $y$  direction at a strain rate of  $0.01\% \text{ ps}^{-1}$ . The results are shown in the left panel of Fig. 3.

It is possible to see that  $\varepsilon_x$  increases with  $\varepsilon_y$ , which is the signature of a negative Poisson's ratio and consequently of the auxetic behavior. The rate of increase of  $\varepsilon_x$  is slow for low  $\varepsilon_y$ , but it suddenly increases. The average Poisson's ratio estimated for  $\varepsilon_x = 4\%$  is -0.91. The same test was simulated, now pulling the structure along the  $x$  direction. The obtained average value of the Poisson's ratio is about -0.30. This result confirms the auxeticity of a finite sample of  $A\gamma G$  structure at room temperature. The results are numerically different from that of an infinite network because the boundary conditions on the structure (which opposes the lateral expansion) are different, and the interactions between the  $A\gamma G$  structure and the substrate can influence its deformation mechanisms. Videos of these simulations (videos S3 and S4) are also shown in supplementary material.

#### 4. Conclusions

In summary, a new auxetic structure, based on the densest  $\gamma$ -graphyne structure, here named  $A\gamma G$  structure, is proposed and its mechanical and electronic properties analyzed using classical reactive and

quantum molecular dynamics simulations. We found that A $\gamma$ G has a large bandgap of 2.48 eV, which will prevent electronic excitation coming from low-energy thermal or optical interactions. Its thermal stability was validated with the different adopted methods. From the mechanical point of view, it presents a low Young’s modulus value when compared to that of graphene or even to that of  $\gamma$ -graphyne (about 300 and 163 GPa.nm [30], respectively). This result is expected since the A $\gamma$ G structure consists of a  $\gamma$ -graphyne structure with several acetylenic chains/arms removed. Our results show that the A $\gamma$ G is auxetic both when isolated (vacuum) and when deposited on a copper substrate. We believe that this is the densest auxetic structure belonging to the graphyne-like families.

## 5. ACKNOWLEDGMENTS

Authors acknowledge support from the Brazilian agencies FAPESP (grants #2013/08293-7, #2018/03961-5 and #2020/02044-9) and CNPq (grants #437034/2018-6, #310369/2017-7 and #311587/2018-6). MJC, DSG, and TJS would like to thank the National Institute for Science and Technology on Organic Electronics (CNPq 573762/2008-2 and FAPESP 2008/57706-4). The authors acknowledge support from the John David Rogers Computing Center (CCJDR) at the Institute of Physics “Gleb Wataghin”, University of Campinas. Part of the computational resources was also provided by the National Laboratory for Scientific Computing, LNCC/MCTIC(LNCC/SantosDumont).

## References

- [1] K. E. Evans, K. Alderson, Auxetic materials: the positive side of being negative, *Engineering Science & Education Journal* 9 (2000) 148–154(6). doi:10.1049/esej\_20000402.
- [2] K. E. Evans, A. Alderson, Auxetic materials: Functional materials and structures from lateral thinking!, *Advanced Materials* 12 (9) (2000) 617–628. doi:10.1002/(SICI)1521-4095(200005)12:9<617::AID-ADMA617>3.0.CO;2-3.
- [3] G. N. Greaves, Poisson’s ratio over two centuries: challenging hypotheses, *Notes and Records: the Royal Society Journal of the History of Science* 67 (1) (2013) 37–58. doi:10.1098/rsnr.2012.0021.
- [4] K. E. Evans, M. A. Nkansah, I. J. Hutchinson, S. C. Rogers, Molecular network design, *Nature* 353 (6340) (1991) 124–124. doi:10.1038/353124a0.
- [5] R. Lakes, Foam structures with a negative Poisson’s ratio, *Science* 235 (4792) (1987) 1038–1040. doi:10.1126/science.235.4792.1038.
- [6] R. Lakes, Advances in negative Poisson’s ratio materials, *Advanced Materials* 5 (4) (1993) 293–296. doi:/10.1002/adma.19930050416.
- [7] R. H. Baughman, D. S. Galvão, Crystalline networks with unusual predicted mechanical and thermal properties, *Nature* 365 (6448) (1993) 735–737. doi:10.1038/365735a0.
- [8] W. Wang, C. He, L. Xie, Q. Peng, The temperature-sensitive anisotropic negative Poisson’s ratio of carbon honeycomb, *Nanomaterials* 9 (4) (2019) 487. doi:10.3390/nano9040487.
- [9] S. P. Silva, M. A. Sabino, E. M. Fernandes, V. M. Correlo, L. F. Boesel, R. L. Reis, Cork: properties, capabilities and applications, *International Materials Reviews* 50 (6) (2005) 345–365. doi:10.1179/174328005X41168.

- [10] J. N. Grima, D. Attard, Molecular networks with a near zero Poisson's ratio, *Physica Status Solidi (b)* 248 (1) (2011) 111–116. doi:10.1002/pssb.201083979.
- [11] Y. Wu, N. Yi, L. Huang, T. Zhang, S. Fang, H. Chang, N. Li, J. Oh, J. A. Lee, M. Kozlov, A. C. Chipara, H. Terrones, P. Xiao, G. Long, Y. Huang, F. Zhang, L. Zhang, X. Lepró, C. Haines, M. D. Lima, N. P. Lopez, L. P. Rajukumar, A. L. Elias, S. Feng, S. J. Kim, N. T. Narayanan, P. M. Ajayan, M. Terrones, A. Aliev, P. Chu, Z. Zhang, R. H. Baughman, Y. Chen, Three-dimensionally bonded spongy graphene material with super compressive elasticity and near-zero Poisson's ratio, *Nature Communications* 6 (2015) 6141. doi:10.1038/ncomms7141.
- [12] V. Gaal, V. Rodrigues, S. O. Dantas, D. S. Galvão, A. F. Fonseca, New zero poisson's ratio structures, *Physica Status Solidi (RRL) – Rapid Research Letters* 14 (3) (2020) 1900564. doi:10.1002/pssr.201900564.
- [13] J.-W. Jiang, S. Y. Kim, H. S. Park, Auxetic nanomaterials: Recent progress and future development, *Applied Physics Reviews* 3 (4) (2016) 041101. doi:10.1063/1.4964479.
- [14] B. Mortazavi, M. Shahrokhi, M. Makaremi, T. Rabczuk, Anisotropic mechanical and optical response and negative poisson's ratio in Mo<sub>2</sub>C nanomembranes revealed by first-principles simulations, *Nanotechnology* 28 (11) (2017) 115705. doi:10.1088/1361-6528/aa5c29.
- [15] L. J. Gibson, M. F. Ashby, G. S. Schajer, C. I. Robertson, The mechanics of two-dimensional cellular materials, *Proceedings of the Royal Society of London. A. Mathematical and Physical Sciences* 382 (1782) (1982) 25–42. doi:10.1098/rspa.1982.0087.
- [16] K. Wojciechowski, Constant thermodynamic tension Monte Carlo studies of elastic properties of a two-dimensional system of hard cyclic hexamers, *Molecular Physics* 61 (5) (1987) 1247–1258. doi:10.1080/00268978700101761.
- [17] M. A. Nkansah, K. E. Evans, I. J. Hutchinson, Modelling the mechanical properties of an auxetic molecular network, *Modelling and Simulation in Materials Science and Engineering* 2 (3) (1994) 337–352. doi:10.1088/0965-0393/2/3/004.
- [18] K. E. Evans, A. Alderson, F. R. Christian, Auxetic two-dimensional polymer networks. an example of tailoring geometry for specific mechanical properties, *J. Chem. Soc., Faraday Trans.* 91 (1995) 2671–2680. doi:10.1039/FT9959102671.
- [19] C. He, P. Liu, A. C. Griffin, Toward negative Poisson ratio polymers through molecular design, *Macromolecules* 31 (9) (1998) 3145–3147. doi:10.1021/ma970787m.
- [20] J. N. Grima, K. E. Evans, Self expanding molecular networks, *Chem. Commun.* (2000) 1531–1532. doi:10.1039/B004305M.
- [21] J. N. Grima, D. Attard, R. N. Cassar, L. Farrugia, L. Trapani, R. Gatt, On the mechanical properties and auxetic potential of various organic networked polymers, *Molecular Simulation* 34 (10-15) (2008) 1149–1158. doi:10.1080/08927020802512187.
- [22] Y. Suzuki, G. Cardone, D. Restrepo, T. S. Zavattieri, Pablo D. Baker, F. A. Tezcan, Self-assembly of coherently dynamic, auxetic, two-dimensional protein crystals, *Nature* 533 (7603) (2016) 369–373. doi:10.1038/nature17633.
- [23] M. Li, K. Yuan, Y. Zhao, Z. Gao, X. Zhao, A novel hyperbolic two-dimensional carbon material with an in-plane negative Poisson's ratio behavior and low-gap semiconductor characteristics, *ACS Omega* 5 (26) (2020) 15783–15790. doi:10.1021/acsomega.0c00182.
- [24] R. H. Baughman, H. Eckhardt, M. Kertesz, Structure-property predictions for new planar forms of carbon: Layered phases containing sp<sup>2</sup> and sp atoms, *The Journal of Chemical Physics* 87 (11) (1987) 6687–6699. doi:10.1063/1.453405.
- [25] A. Ivanovskii, Graphynes and graphdienes, *Progress in Solid State Chemistry* 41 (1) (2013) 1–19. doi:10.1016/j.progsolidstchem.2012.12.001.
- [26] Y. Li, L. Xu, H. Liu, Y. Li, Graphdiyne and graphyne: from theoretical predictions to practical construction, *Chem. Soc. Rev.* 43 (2014) 2572–2586. doi:10.1039/C3CS60388A.
- [27] D. Malko, C. Neiss, F. Viñes, A. Görling, Competition for graphene: Graphynes with direction-dependent dirac cones, *Phys. Rev. Lett.* 108 (2012) 086804. doi:10.1103/PhysRevLett.108.086804.
- [28] X.-M. Wang, D.-C. Mo, S.-S. Lu, On the thermoelectric transport properties of graphyne by the first-principles method,



- The Journal of Chemical Physics 138 (20) (2013) 204704. doi:10.1063/1.4806069.
- [29] H. Sevincli, C. Sevik, Electronic, phononic, and thermoelectric properties of graphyne sheets, *Applied Physics Letters* 105 (22) (2014) 223108. doi:10.1063/1.4902920.
- [30] S. A. Hernandez, A. F. Fonseca, Anisotropic elastic modulus, high Poisson's ratio and negative thermal expansion of graphynes and graphdiynes, *Diamond and Related Materials* 77 (2017) 57–64. doi:10.1016/j.diamond.2017.06.002.
- [31] S. W. Cranford, M. J. Buehler, Mechanical properties of graphyne, *Carbon* 49 (13) (2011) 4111–4121. doi:10.1016/j.carbon.2011.05.024.
- [32] D. Galhofo, N. Silvestre, Computational simulation of  $\gamma$ -graphynes under monotonic and hysteretic loading, *Mechanics of Advanced Materials and Structures* 28 (5) (2021) 495–505. doi:10.1080/15376494.2019.1578007.
- [33] Y. Yang, Q. Cao, Y. Gao, S. Lei, S. Liu, Q. Peng, High impact resistance in graphyne, *RSC Adv.* 10 (2020) 1697–1703. doi:10.1039/C9RA09685J.
- [34] S. Plimpton, Fast parallel algorithms for short-range molecular dynamics, *Journal of Computational Physics* 117 (1) (1995) 1–19. doi:10.1006/jcph.1995.1039.
- [35] R. C. Andrew, R. E. Mapasha, A. M. Ukpong, N. Chetty, Mechanical properties of graphene and boronitrene, *Phys. Rev. B* 85 (2012) 125428. doi:10.1103/PhysRevB.85.125428.
- [36] D. W. Brenner, O. A. Shenderova, J. A. Harrison, S. J. Stuart, B. Ni, S. B. Sinnott, A second-generation reactive empirical bond order (REBO) potential energy expression for hydrocarbons, *Journal of Physics: Condensed Matter* 14 (4) (2002) 783–802. doi:10.1088/0953-8984/14/4/312.
- [37] T. Liang, T.-R. Shan, Y.-T. Cheng, B. D. Devine, M. Noordhoek, Y. Li, Z. Lu, S. R. Phillpot, S. B. Sinnott, Classical atomistic simulations of surfaces and heterogeneous interfaces with the charge-optimized many body (COMB) potentials, *Materials Science and Engineering: R: Reports* 74 (9) (2013) 255–279. doi:10.1016/j.mser.2013.07.001.
- [38] A. C. T. van Duin, S. Dasgupta, F. Lorant, W. A. Goddard, Reaxff: A reactive force field for hydrocarbons, *The Journal of Physical Chemistry A* 105 (41) (2001) 9396–9409. doi:10.1021/jp004368u.
- [39] J. E. Mueller, A. C. T. van Duin, W. A. Goddard, Development and validation of Reaxff reactive force field for hydrocarbon chemistry catalyzed by nickel, *The Journal of Physical Chemistry C* 114 (11) (2010) 4939–4949. doi:10.1021/jp9035056.
- [40] D. Porezag, T. Frauenheim, T. Kohler, G. Seifert, R. Kaschner, Construction of tight-binding-like potentials on the basis of density-functional theory: Application to carbon, *Physical Review B* 51 (1995) 12947.
- [41] G. Seifert, D. Porezag, T. Frauenheim, Calculations of molecules, clusters, and solids with a simplified LCAO-DFT-LDA scheme, *Int. J. Quantum Chemistry* 58 (1996) 185.
- [42] H. Manzano, A. N. Enyashin, J. S. Dolado, A. Ayuela, J. Frenzel, G. Seifert, Do cement nanotubes exist?, *Advanced Materials* 24 (24) (2012) 3239–3245. doi:10.1002/adma.201103704.
- [43] P. Koskinen, V. Mäkinen, Density-functional tight-binding for beginners, *Computational Materials Science* 47 (1) (2009) 237–253.
- [44] M. Elstner, D. Porezag, G. Jungnickel, J. Elsner, M. Haugk, T. Frauenheim, S. Suhai, G. Seifert, Self-consistent-charge density-functional tight-binding method for simulations of complex materials properties, *Physical Review B* 58 (11) (1998) 7260–7268. doi:10.1103/PhysRevB.58.7260.
- [45] B. Aradi, B. Hourahine, T. Frauenheim, DFTB+, a sparse matrix-based implementation of the DFTB method, *The Journal of Physical Chemistry A* 111 (26) (2007) 5678–5684. doi:10.1021/jp070186p.
- [46] S. Gemming, A. N. Enyashin, J. Frenzel, G. Seifert, Adsorption of nucleotides on the rutile (110) surface, *International Journal of Materials Research* 101 (6) (2010) 758–764. doi:10.3139/146.110337.
- [47] B. Lukose, A. Kuc, J. Frenzel, T. Heine, On the reticular construction concept of covalent organic frameworks, *Beilstein Journal of Nanotechnology* 1 (2010) 60–70. doi:10.3762/bjnano.1.8.
- [48] T. Kubar, Z. Bodrog, M. Gaus, C. Koehler, B. Aradi, T. Frauenheim, M. Elstner, Parametrization of the SCC-DFTB

- method for halogens, *Journal of Chemical Theory and Computation* 9 (7) (2013) 2939–2949. doi:10.1021/ct4001922.
- [49] D. J. Evans, B. L. Holian, The nose–hoover thermostat, *The Journal of chemical physics* 83 (8) (1985) 4069–4074.
- [50] W. Humphrey, A. Dalke, K. Schulten, VMD: Visual molecular dynamics, *Journal of Molecular Graphics* 14 (1) (1996) 33–38. doi:10.1016/0263-7855(96)00018-5.